PHYSICAL REVIEW E **74**, 045202(R) (2006)

Noise-induced intermittent cellular patterns on circular domains

Peter Blomgren,* Scott Gasner,† and Antonio Palacios‡
Nonlinear Dynamics Group, Department of Mathematics and Statistics, San Diego State University, San Diego, California 92182-7720, USA

(Received 20 December 2005; revised manuscript received 8 August 2006; published 25 October 2006)

We study the effects of thermal noise in a stochastic Langevin formulation of a typical example of a pattern-forming system with two-dimensional circular domain. A greater tendency towards dynamic cellular states is observed when the pattern-forming system is subjected to noise, which seems to explain the prevailing behavior of related laboratory experiments. We also report on two-dimensional numerical observations of certain dynamic states, homoclinic intermittent states, which until now, had only been observed in laboratory experiments.

DOI: 10.1103/PhysRevE.74.045202 PACS number(s): 05.40.−a, 02.60.Cb, 05.45.−a, 47.54.−r

Cellular patterns are common features of many nonlinear phenomena. In material science, they are observed in polycrystalline metals, soap suds, bubbles in lipid monolayers, bubbles in fluidization and solidification processes, and magnetic bubbles [1]. They are also found in biological [2] and in vibrated granular systems [3]. Understanding the mechanisms that govern the spatial and temporal evolution of cellular patterns, and their response to noise, is important because such knowledge can lead, for instance, to novel designs and developments of new materials. With this perspective in mind, we investigate the effects of noise in a stochastic (Langevin) version of a typical example of a cellular-pattern-forming dynamical system, known as the Kuramoto-Sivashinsky (KS) equation

$$\frac{\partial u}{\partial t} = \eta_1 u - (1+\nabla^2)^2 u - \eta_2(\nabla u)^2 - \eta_3 u^3 + \xi(\vec{x},t), \quad (1)$$

where $u=u(\vec{x},t)$ represents the perturbation of a planar front (typically assumed to be a flame front) by thermodiffusive instabilities in the direction of propagation. In Eq. (1), η_1 measures the strength of the perturbation force, η_2 is a parameter associated with growth in the direction normal to the circular domain (burner), $\eta_3 u^3$ is a term that is added [4] to help stabilize the numerical integration, and $\xi(\vec{x},t)$ represents Gaussian white noise, which models thermal fluctuations, dimensionless in space and time. We assume $\xi(\vec{x},t)$ to be distributed with zero mean $\langle\xi(\vec{x},t)\rangle=0$, and to be uncorrelated over space and time, i.e., $\langle\xi(\vec{x},t)\xi(\vec{x}',t')\rangle=2D\delta(\vec{x}-\vec{x}')\delta(t-t')$, where D is a measure of the intensity of the noise, $\langle\cdots\rangle$ represents the time average over a range of observations.

The Kuramoto-Sivashinsky equation has been studied in different contexts by Cross and Hohenberg [5], Armbruster, Guckenheimer, and Holmes [6], and by Palacios *et al.* [7]. These studies show that, overall, thermodiffusive instabilities can lead to complex stationary and dynamic cellular patterns, which emerge from the geometry of the domain through the universal properties of symmetry-breaking bifurcations. In recent work [8], we developed a Crank-Nicolson based integration scheme that solves a numerical instability problem of the first truly two-dimensional numerical integration scheme developed by Zhang *et al.* [9]. In the present study we build on this numerical scheme in order to study the effects of noise on the formation of cellular patterns. Computer simulations of Eq. (1) shows a predominant tendency towards stationary states, in the absence of noise. In the presence of noise, the preferred patterns are, however, dynamic states. We also report on the two-dimensional numerical observation of certain intermittent states, some of which had only been observed, until now, in laboratory experiments. Similar results have been studied in the context of turbulence [10]; theoretical and simulation results are available for the one-dimensional (1D) KS equation [11].

Numerical method. The numerical scheme used to integrate the stochastic version of the KS model (1) employs distributed approximating functionals for calculating the spatial derivatives [8,9,12]. Time integration is Crank-Nicolson based [13], second order accurate, and linearly unconditionally A stable. The nonlinearities are handled by Newton iteration in each time step, where the resulting sequence of linear systems are solved using the preconditioned Bi-CGSTAB method [14]. The preconditioner is chosen to be the unchanging linear part of the discretized operator. The stochastic contribution to the system $\xi(\vec{x},t)$ only affects the linear systems in the form of a constant, over each time step, addition to the right-hand side.

Simulations. Computer simulations of the KS model (1) show an increased propensity for stationary over dynamic states, whenever noise is absent. The former states are ordered states with petal-like cellular structures and well-defined spatial symmetries, see Fig. 1. As the radius of the circular domain increases, the ordered states undergo various symmetry-breaking bifurcations, which increase the complexity of the patterns; more cells form, and eventually additional concentric rings of cells appear.

Dynamic states are sometimes observed in the transition region between two stationary states. In previous work [7], we studied the selection mechanism in this transition. We now study the effects of noise on these transitions. Under noise-free conditions, corresponding to $D=0$ in the bifurcation diagram of Fig. 2, a dynamic one-cell rotating (1R) state appears in a very narrow range of radii, between the one-cell (1S) and the two-cell stationary (2S) states, i.e., a 1-to-2 mode interaction. The shape of the single rotating cell resembles the 1S state (i.e., Fig. 1, panel 1).

*Electronic mail: blomgren@terminus.sdsu.edu
†Electronic mail: sgasner@yahoo.com
‡Electronic mail: palacios@euler.sdsu.edu

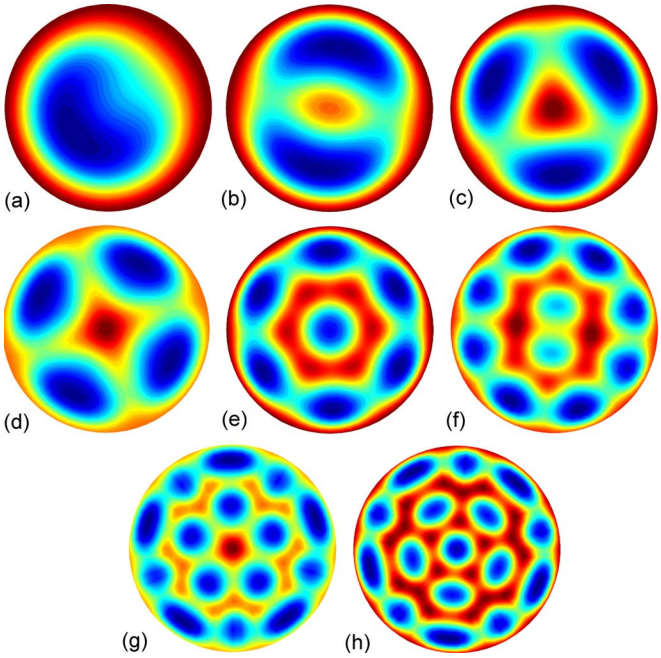

FIG. 1. (Color online) Samples of stationary states found through numerical simulations of the KS model (1) without noise. The cells organize in concentric rings, with an increasing number of cells in the outer rings. The cell sizes within each pattern are approximately constant. The radii corresponding to the panels are [4.2, 5.0, 6.0, 8.0] and [8.625, 11.0, 13.75, 14.0]; with the simulation parameters $(\eta_1, \eta_2, \eta_3)=(0.32, 1.0, 0.17)$ being identical for all eight simulations.

In order to get insight into the effects of noise, we focus our attention around this 1-to-2 mode interaction that leads to a 1R-state, though the analysis still captures many essential features of the effects of noise on more complex patterns. With increasing noise intensity, the range of radii yielding 1R-states is extended, and *additional* patterns emerge, see Fig. 2. For very weak noise, an unsteady dynamic pattern (1U) appears between the 1S and 1R states. The 1U pattern, similar in shape to the 1R state, does not sustain rotations; instead, it visibly rocks back and forth. Increasing the noise intensity further leads to the formation of a one-cell rotating pattern which *intermittently* changes its direction of rotation; this pattern is observed between the 1U and 1R patterns, we denote this pattern by (1RI) in the bifurcation diagram. At this noise level we now have a 1S-1U-1RI-1R-2S transition.

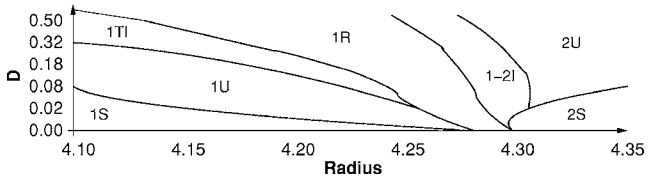

FIG. 2. Schematic behavior of the KS model for various parameter values of radius and noise intensity. Notation: 1=single cell, 2=two cells. S=stationary, U=unsteady, RI=rotating intermittent, R=rotating, 1-2I=1/2-cell intermittent (heteroclinic cycle). Noise levels are actually low noise levels since the dynamic range of u in the Kuramoto-Sivashinsky equation is order 10. Beyond $D=1.25\times10^{-3}$ no static patterns are observed.

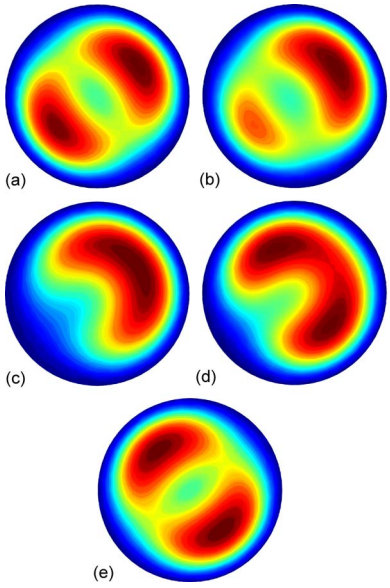

FIG. 3. (Color online) Representative snapshots of simulations of the KS model with simulation parameters $R=4.285$, $D=0.0008$, and $\eta_{1,2,3}$ as in Fig. 1. Here we see the 1-2I state, in which extinction and subsequent reformation of the second cell occurs at intermittent intervals.

Between the 1R and 2S (or, for higher noise intensities, 2U) patterns, an intermittent 1-2 cell pattern forms, representative snapshots are shown in Fig. 3. This dynamic pattern is very peculiar: one of the two cells in the 2S state is extinguished; the remaining one-cell state is short-lived, the pattern immediately splits into a new 2S state, the orientation of which is roughly a quarter rotation of the previous 2S state. Each appearance of the 2S state lasts an irregular amount of time, ranging from a few to several hundreds of frames. This is qualitative evidence of a heteroclinic connection where the stable (unstable) manifold of a two-cell equilibrium is also the unstable (stable) manifold of another two-cell equilibrium. Until now, this pattern had only been observed in laboratory experiments [15,16] but not in 2D simulations of the KS model. Finally, a two-cell analog 2U of the 1U pattern forms between the 1-2I and 2S patterns.

Analysis. In order to explain, quantitatively, the origin and formation mechanisms of the noise-induced dynamic patterns that we described above, we consider the influence of noise on the normal form equations for a 1-to-2 cell mode interaction in a system with $O(2)$ symmetry, i.e., the symmetry group of rotations and reflections of the circular domain. Projecting the KS equation (1) onto Fourier-Bessel modes, we obtain (after rescaling) the desired normal forms

$$\dot{z}_1 = \bar{z}_1 z_2 + z_1(\mu_1 + e_{11}|z_1|^2 + e_{12}|z_2|^2) + \varepsilon g(t),$$

$$\dot{z}_2 = \pm z_1^2 + z_2(\mu_2 + e_{21}|z_1|^2 + e_{22}|z_2|^2) + \varepsilon h(t), \qquad (2)$$

where $g(t)$ and $h(t)$ are Gaussian white noise functions, uncorrelated with zero mean, with amplitude ε. The two-parameter bifurcation diagram for the noise-free case, i.e., $D=0$, shown in Fig. 4 indicates the region of existence and stability of related patterns (see Refs. [6,17]).

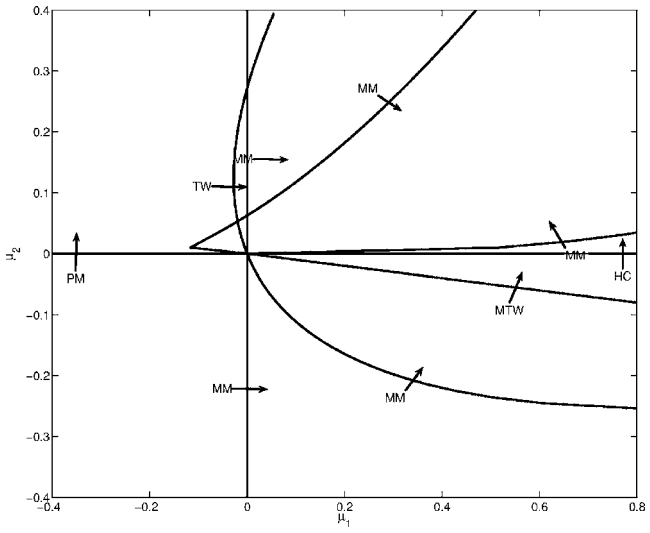

FIG. 4. Two-parameter bifurcation diagram of the KS equation (1). Notation: PM=pure modes, MM=mixed modes, TW=traveling waves, MTW=modulated traveling waves, HC=heteroclinic cycles. Arrows indicate direction by which a given solution becomes stable.

The deterministic version of the normal forms (2) has been thoroughly studied by Armbruster *et al.* [17]. The Langevin version where $g(t)$ and $h(t)$ are Gaussian white noise functions, uncorrelated with zero mean, with amplitude ε, has also been studied (with particular emphasis on the effects of noise on heteroclinic connections) by Stone and Holmes [18]. Among their findings, most relevant to this work, is the realization that intermittent states are noise-induced "stochastic limit cycles" that are created from the perturbation of heteroclinic orbits connecting saddle-node equilibria of the deterministic ($\varepsilon=0$) normal forms. The passage time of a typical orbit lingering near one of these equilibrium points obeys the following probability distribution function

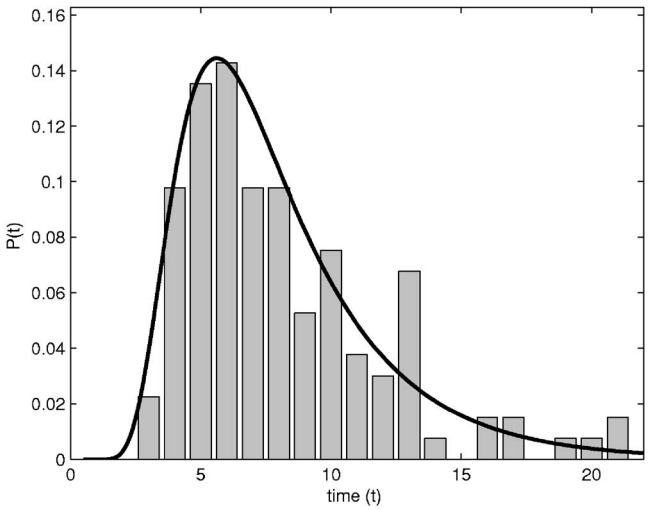

FIG. 5. Passage times calculated (vertical bars) from numerical simulations of the 1-2I intermittent pattern and (bold curve) by fitting the probability distribution function of Eq. (3) with parameters $\lambda=0.28$, $\varepsilon=0.030$, and $\delta=0.20$.

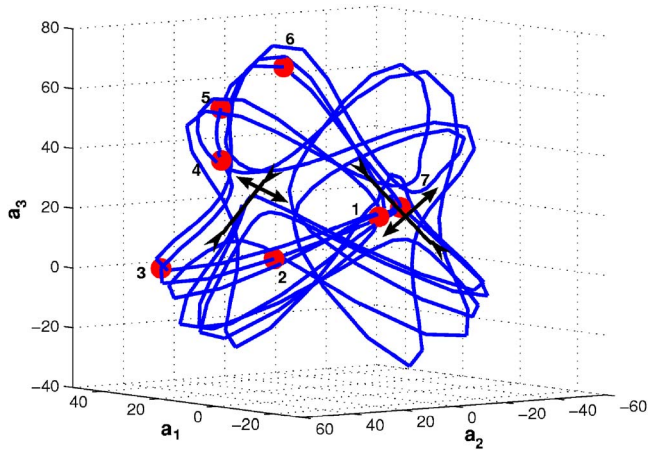

FIG. 6. (Color online) The phase space corresponding to the first three empirical orthogonal basis functions for the snapshot sequence of the 1-2I simulation of the KS model with simulation parameters as in Fig. 3. We clearly see the saddle-node connections between the stable and unstable manifolds associated with each individual ordered pattern, one with one cell and one with two cells.

$$P(t) = \frac{2\lambda\Delta(t)e^{-\Delta^2(t)}}{\sqrt{\pi}(1-e^{-2\lambda t})}, \tag{3}$$

where $\Delta(t)=\delta[(\varepsilon^2/\lambda)(e^{2\lambda t}-1)]^{-1/2}$, λ is the largest unstable eigenvalue of the equilibrium points, ε is the noise amplitude seen in Ref. (2), and δ is the size of a neighborhood around the equilibrium points. In Fig. 5 we calculate the passage times (vertical bars) for the numerical simulations of the 1-2I pattern of Fig. 3. The equilibrium points correspond to the two different orientations of the two-cell states that appear intermittently. The bold curve is a fitting of the probability distribution function $P(t)$ given by Eq. (3).

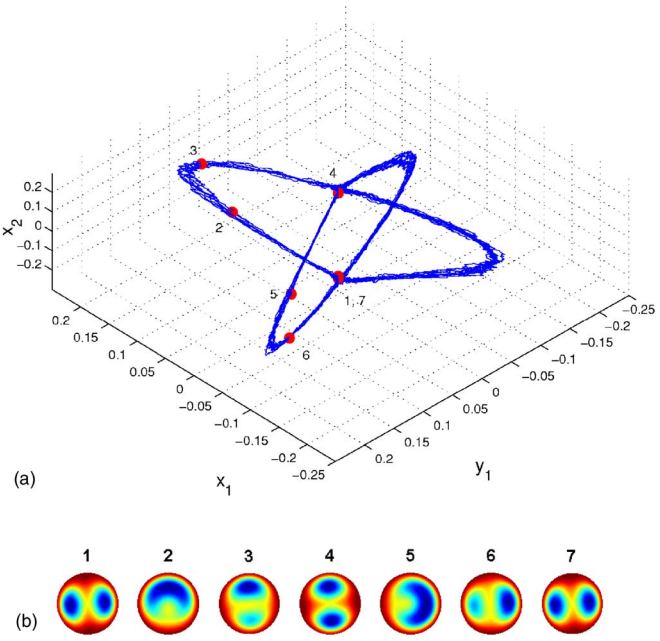

FIG. 7. (Color online) Phase-space reconstruction of the 1-2I state of Fig. 3 via solutions of normal form equations (2).

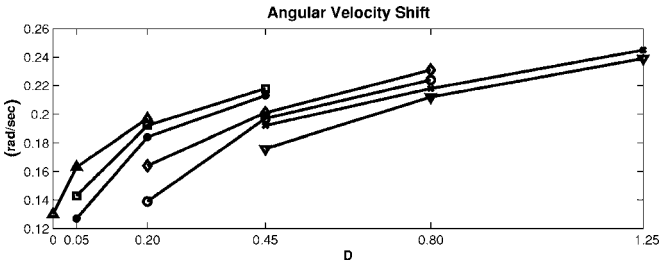

FIG. 8. Angular velocity in single cell rotations (1R) measured in rad/s as a function of noise intensity. Each line represents a series of simulations in which all parameters were held constant except for noise intensity (range $[0, 1.25\times10^{-3}]$).

Together, (i) the numerical calculations yielding the curve fitting of $P(t)$; (ii) the close structural correspondence of the phase-spaces related to the KS simulation (Fig. 6) and the normal form simulation (Fig. 7, top panel); as well as (iii) the matching of the reconstruction of the dynamics described by the normal form simulation (Fig. 7, bottom panels) to KS-simulation behavior (Fig. 3); are all strong indicators that the 1-2I intermittent state is indeed a stochastic limit cycle created from the perturbation of a heteroclinic connection. Such connections would be unobservable in the 2D simulation under noise-free conditions.

We have now extended the analysis of Stone and Holmes [18] of the Langevin normal forms (2) to other regions of parameter space where other dynamic patterns, beyond heteroclinic cycles, exist. We summarize the results next but details of the analysis can be found in an companion publication [19]. A mode analysis (via proper orthogonal decomposition and Fourier-Bessel decomposition) shows that all three intermittent patterns 1RI, 1U, and 1-2I, emerge from the mutual interaction of two pairs of spatial modes, with wave numbers in a 1:2 ratio. Analysis of the phase dynamics [relative to the rotation of the $O(2)$-symmetry] of the amplitude coefficients associated with the basis modes further reveals a single frequency in the Fourier spectrum of the phase of the 1RI pattern. It is then reasonable to classify the 1RI pattern as a traveling wave solution, subject to noise, of the 1:2 mode interaction. As noise increases, the angular velocity of the 1R and 1RI patterns increases as is shown in Fig. 8.

Similarly, the phase of the 1U (and 2U as well) pattern remains almost constant while it lies in an invariant subspace spanned by a pair of basis Fourier-Bessel modes. This suggests that the 1U (and 2U) state are standing wave patterns in which noise perturbations cause the observed rocking back-and-forth motion. We note that the noise-free dynamic patterns were already stable; noise is not stabilizing these patterns. Instead, it is changing their dynamic characteristics. Again, details of the normal form analysis can be found in an upcoming paper [19]. As a closing remark, we wish to emphasize that more complex intermittent transitions, see Fig. 9, are also found in simulations of the KS model (1). Our analysis of the 1:2 mode interaction can be readily extended, except that some of the normal forms for this and many other cases have not yet been derived.

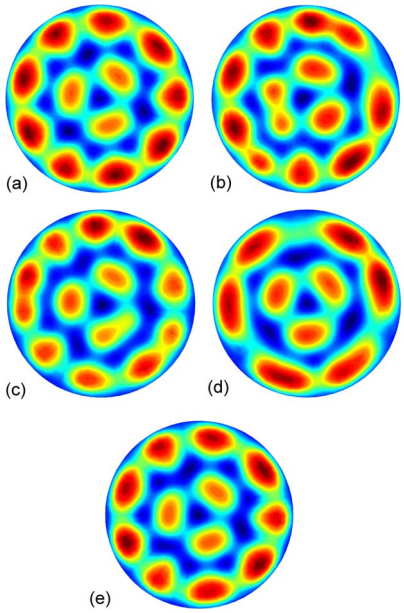

FIG. 9. (Color online) For $R=13.101$, $D=0.00125$, and $\eta_{1,2,3}$ as in Fig. 1, noise-induced intermittent behavior in a two-ring state is observed. Here, the transitions visit 9/3, 9/4, 10/3, 10/4 (not shown), and 6/3 two-ring states at intermittent intervals.

This work has been supported in part by NSF Grants Nos. DMS-0504150 and CHE-0216563.

[1] J. A. Glazier and D. Weaire, J. Phys.: Condens. Matter. **4**, 1867 (1992).
[2] *Pattern Formation in Biology, Vision and Dynamics*, edited by A. Carbone *et al.* (World Scientific, Singapore, 1998).
[3] L. S. Tsimring and I. S. Aranson, Phys. Rev. Lett. **79**, 213 (1997).
[4] H. Chaté and B. Nicolaenko, in *New Trends in Nonlinear Dynamics and Pattern Forming Phenomena* (Plenum, New York, 1990).
[5] M. C. Cross and P. C. Hohenberg, Rev. Mod. Phys. **65**, 851 (1993).
[6] D. Armbruster *et al.*, SIAM J. Appl. Math. **49**, 676 (1989).
[7] A. Palacios *et al.*, Chaos **7**, 463 (1997).
[8] P. Blomgren *et al.*, Phys. Rev. E **72**, 036701 (2005).
[9] D. S. Zhang *et al.*, Phys. Rev. E **60**, 3353 (1999).
[10] N. Aubry *et al.*, J. Fluid Mech. **192**, 115 (1988).
[11] I. G. Kevrekidis *et al.*, SIAM J. Appl. Math. **50**, 760 (1990).
[12] P. Blomgren *et al.*, Chaos **15**, 013706 (2005).
[13] J. Crank and P. Nicolson, Proc. Cambridge Philos. Soc. **43**, 50 (1947).
[14] H. A. van der Vorst, SIAM (Soc. Ind. Appl. Math.) J. Sci. Stat. Comput. **13**, 631 (1992).
[15] M. Gorman *et al.*, Combust. Sci. Technol. **98**, 79 (1994).
[16] E. Stone *et al.*, Phys. Rev. Lett. **76**, 2061 (1996).
[17] D. Armbruster *et al.*, Physica D **29**, 257 (1988).
[18] E. Stone and P. Holmes, Phys. Lett. A **155**, 29 (1991).
[19] S. Gasner *et al.*, Int. J. Bifurc. Chaos. **17** (2007).